

Simulation and Evaluation of Sensor Characteristics in Vision Based Advanced Driver Assistance Systems

Dennis Hospach, Stefan Mueller, Oliver Bringmann, Joachim Gerlach, Wolfgang Rosenstiel
University of Tuebingen, Faculty of Science, Dept. of Computer Engineering
Email: {dennis.hospach, stefan.mueller}@uni-tuebingen.de

Abstract—This paper presents a method for the simulation of images in the scope of virtual camera prototypes under the constraint of color correctness. This is a first step to gain a complete simulatable camera model that can be used to generate synthetic images using real data. Each real camera system has its own color processing characteristics. Real images recorded with a reference camera model can be computationally simulated as if they have been recorded with another real or virtual camera. The resulting images are transformed to underly the color characteristics of the targeted virtual camera system. Our approach can be used at the design phase of vision-based advance driver assistance systems to verify the exact behaviour under varying optical properties of the optical system and to test and evaluate the overall robustness of the system when color processing changes. It can as well lead to a decision basis for the selection of the hardware to be used. In this paper, we show how cameras can be calibrated and in a second step we evaluate the simulation errors. Finally, we apply our simulation to a traffic sign recognition algorithm and evaluate its behaviour in relation to ground truth data.

I. INTRODUCTION

The steady increase in the performance of system-on-chip (SoC) components by reducing the feature size and the increase of the integration density and the concomitant increase in energy efficiency, made the use of such components more attractive in mobile applications. This trend is also visible in the automotive industry. In today's cars, hundreds of microelectronic chips are used for power train, safety, comfort and infotainment applications and the embedded software content is measured by hundreds of megabytes. Compared to previous vehicle generations that were fitted with a fairly small number of driver assistance systems such as Antilock Braking System (ABS) and Electronic Stability Control (ESC), the variety of driver assistance systems in modern vehicles is much higher. Today's Advanced Drivers Assistance Systems (ADAS) functions like light assistant, lane departure warning system, traffic sign / light recognition up to night vision displayed in the windshield have been implemented. Many of these systems are vision-based and the trend is rising. Also, the current autonomous driving concept cars heavily depend on vision-based systems. The major problem is to guarantee functional safety requirements, especially if advanced driver assistance systems are taking over more and more active control over the vehicle. The development of safety-relevant electrical / electronic / programmable electronic systems is covered by two standards: the basic functional safety standard IEC 61508 and the

ISO 26262 as an adaption for the automotive domain. Both standards recommend the use of a failure mode and effect analysis (FMEA) to reveal faults and the resulting effects. In order to incorporate FMEA in the early development states, the use of virtual prototypes is essential. The stimulation of the virtual prototype is defined by the input of the ADAS systems which usually consist of video, radar, LiDAR or ultrasonic sensors which need to be modeled as well. However, these systems have to operate correctly in very different environmental conditions which are strongly influenced by the traffic situation, weather conditions, illumination, etc. This requires a huge amount of on-road captures to test all combinations of environmental influences. Nevertheless, a total coverage is unrealistic. This paper presents a method for the simulation of color processing of optical virtual prototypes and therefore closes the gap between the simulation of the cyber part and the physical world. With the presented methods it is possible to test combinations of multiple optical sensors with ADAS algorithms and evaluate their behaviour with respect to color characteristics as early as at the design stage.

II. RELATED WORK

The challenges in safety evaluation of automotive electronic using virtual prototypes is stated in [1]. Most vision-based ADAS techniques heavily rely on machine learning algorithms, such as neural networks and support vector machines (SVM) as presented in [2], [3] and / or bayesian networks [3]. All these approaches have in common that they need to be trained with well selected training data [4], [5]. There are approaches to generate synthetic training data, where image degradation [6] or characteristics of the sensor and the optical system [7] are used to enlarge the training data. Most ADAS employ several sensors, networks and Electrical Control Units (ECU) to fulfill their work, which results in a complex scenario that can be considered as a Cyber-Physical System (CPS) [8]. A methodology to generate virtual prototypes from such large systems while keeping a maintainable speed is shown in [9]. It uses different abstraction levels to reach high performance of the controller and network models which are connected to a physical environment simulation. Another paper that covers virtual prototyping in the scope of ADAS was presented by Reiter et al [10]. They show, how robustness and error tolerance of ADAS can be improved with error effect simulation.

Very basic insights on how the transportation of light and the formation of images works come from [11] and [12]. In [13], Debevec and Malik show how the incident irradiance at the sensor can be reconstructed using the response function of the optical system. With some adaptations, the reconstructed irradiance can be used to simulate another color processing. In [14] Kolb et. al propose a physically based camera model to correctly model the transport of light through the optical parts of a camera and the calculation of images from known irradiance. Finally, [15], [16] and [17] deal with methods to convincingly merge real and virtual scenes which is also related to some of the tasks of this paper.

III. SIMULATED CAMERAS AS A CYBER-PHYSICAL SYSTEM

By definition, a Cyber-Physical Systems consists of sensors which perceive the physical environment and communicate their information to a cyber part - an embedded system - to process this information. Accordingly, we can consider ADAS, which collect environmental data and process them in one or more ECUs to derive suggestions or driving strategies, as a CPS. Very common sensors in the range of ADAS are cameras.

Depending on its specifications, a camera offers e.g. autofocus, automatic white balance, automatic exposure, etc. which are all controlled by an embedded system. A camera itself could also be considered as a CPS, but in the following, we consider cameras as a sensor of an ADAS. For virtual prototyping of ADAS, it is important to evaluate all possible influences on the system. Each of the sensors of such a CPS severely influences the performance of the overall system, as each sensor reacts differently to environmental conditions. These conditions obviously can affect the scene gathered through the camera directly by changing the brightness, contrast and / or depth of field. Furthermore they may exert indirect influence, for example through drifts of the characteristic curve caused by different temperatures.

A. Sensor characteristics

Optical sensors are constructed in a way, such that they show similar behaviour as analog film. The digital quantization of scene radiance introduces new parameters for sensors though. Each of them has more or less influence on the outcome of the imaging process of a digital camera. In order to simulate a sensor, these factors have to be attended.

Digital sensors have a fixed amount of light-sensitive elements (pixels), that are mounted on a chip. The horizontal and vertical amount of these light-sensitive elements determines the resolution of the resulting images. Each pixel may be realized as charge coupled device (CCD) or in CMOS technology. In any case, the incident light is proportional to the analog-to-digital converted charge value. Each pixel is being hit by light from multiple directions and the incident light may contain large parts of the visible spectrum. For color images, digital cameras have to record the red, green and blue components of the light. Since the pixels are sensitive to the whole visible spectrum, a color filter is put in

front of each pixel such that is only transmissive to the red, green or blue parts of the spectrum. Indeed, a pixel for red color information is not only responsive to a sharply defined area around 700 nm wavelength, but rather over the whole spectrum. The intensity of reaction of a pixel to the different parts of the spectrum is called the spectral response.

During the analog-to-digital conversion process some noise is introduced to the pixel values. This is a well-known effect that occurs at all stages of electronic signal processing. Sensor noise can be thought of a statistical shift of the signal value from its perfect ground truth. Each sensor has its own noise behaviour and therefore noise is a characteristic parameter of each sensor. For simulation purposes, it is important to note that if the data of the reference system is low-noise, the noise behaviour of a sensor with high noise level may be calculated and artificial images of the simulated camera may be generated. If the reference system contains heavy noise, it is difficult to get rid of it, though.

The electronic components that process the signal have a varying output when the temperature changes. This effect usually is weak, but if the region of working temperature is large this may become noticeable.

There are lots of parameters to take care of. This paper focuses specifically on the color correctness of the simulation, thus the spectral response and the color balance of the color channels have to be considered here. The other effects will continuously be investigated to fortify the whole simulation process.

B. Simulation of virtual cameras

To simulate the behaviour of a camera, it is necessary to first understand the digital image formation process. In the moment when the trigger button of a camera is pushed, light from the scene is falling through the objective and the aperture onto the sensor backplane. Here it is registered and then converted into a proportional voltage value. It is then being (often nonlinearly) mapped to a pixel value in the final image. This nonlinear mapping is introduced to account for the high dynamic range many natural scenes are showing. In order to be able to digitize a wider range of the scene light, the lower and the upper areas of illumination are compressed stronger.

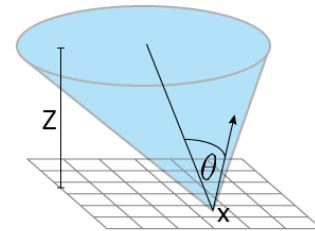


Fig. 1. The geometric relation between incident radiance and sensor irradiance

Sensor irradiance and scene radiance have a direct dependency to each other. Radiometry states that the radiance $L(x', x)$ falling through the entrance pupil at x' and the

irradiance $E(x)$ focusing at a point x on the sensor plane are related through ([14])

$$E(x) = \frac{1}{Z^2} \int L(x', x) \cos^4 \theta dx' \quad (1)$$

where Z is the distance from the sensor plane to the exit pupil and θ is the angle between the sensor plane normal and the ray direction. If we assume that the entrance pupil subtends only a small solid angle, θ can be considered constant and we get a direct relationship between sensor irradiance and integrated scene radiance as

$$E(x) = \frac{1}{Z^2} \cos^4 \theta L(x) \quad (2)$$

where $L(x)$ denotes the integrated scene radiance at x . Figure 1 shows the geometry of this relation.

Additionally, these equations should be considered functions of the wavelength λ . A digital sensor will sample the spectrum typically around three discrete values, one for red, green and blue. Therefore we add an index $[r|g|b]$ to the equations to indicate which discrete color channel is referred to.

As already discussed, the sensor irradiance is mapped to pixel values in a camera specific and most often nonlinear way. In [13], Debevec and Malik present a method to determine this mapping function. First they state, that for the exposure at the sensor only the product of irradiance and exposure time is important. It is defined as

$$X(x) = E(x) * \Delta t \quad (3)$$

The exposure $X(x)$ at point x on the sensor is then mapped to the final pixel value $Z(x)$ by the so-called response curve f . The authors show, that it is reasonable to assume that f is invertible, such that

$$X(x) = f^{-1}(Z(x)) \quad (4)$$

Summarized, we have direct relationships between scene radiance, sensor irradiance, exposure and the final pixel value. To simulate the color characteristic of a virtual camera using images taken with a reference model, we can now follow the path backwards, i.e. from pixel value to exposure, then to irradiance and possibly to scene radiance. Then we can exchange the color characteristics of the reference model with the one of the simulation system and redo the imaging process. Figure 2 summarizes the relations between the different quantities.

Yet, there are a few things to do before we can thread this path. First, we need to talk about how to get the response curve of a sensor, connecting pixel value with exposure. Then we need to take care of the color balance. And finally, the method used by [13] to reconstruct the response curves only yields relative exposure values, valid for only one imaging system. If we'd like to use them with another simulated camera, care needs to be taken on how to remap them.

The first part of the problem, building response curves, is described by Debevec and Malik in detail. They use a series

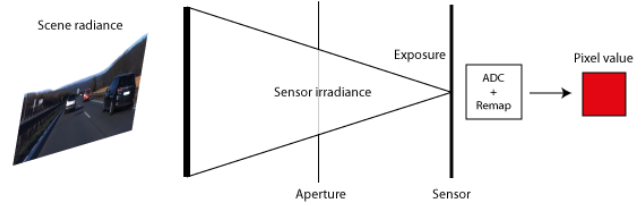


Fig. 2. Quantities in the image formation process

of images taken at different exposure times, from very low to very high exposures. In their next step, they find an optimal solution of the response curve by minimizing a quadratic function under some smoothness terms. However, since they arbitrarily center the response curve by setting unit exposure at a pixel value of 128, this mapping only provides relative information. Further, this method is applied to each color channel separately, leading to three unknown scaling factors for the color channels. So we can formulate the following mathematical equations:

$$X_{[r|g|b]}(x) = f_{[r|g|b]}^{-1}(Z_{[r|g|b]}(x)) \quad (5)$$

$$X'_{[r|g|b]}(x) = \alpha_{[r|g|b]} * X_{[r|g|b]}(x) \quad (6)$$

where $X'_{[r|g|b]}(x)$ denotes the color balanced response curves and $\alpha_{[r|g|b]}$ the correction factors. The latter can be determined by taking images of a series of graylevel fields with known scaling factors of the color channels (e.g. $R = G = B$). These scaling factors should recur at the exposure level and therefore the scaling factors for the response curves can be chosen accordingly. After this step, the calibration of the camera itself is finished. We are now able to simulate pictures taken at different exposure times from one taken picture and we are able to calculate the relative irradiance values from a taken picture.

As stated above, the irradiance values of one camera system are not directly usable in another one. There are two options to convert them. First, the relative sensor irradiance values could be calibrated to absolute scene radiance values using a light meter. By taking images of a diffuse and uniformly lit area of known radiance, the scaling factors between relative sensor irradiance and absolute scene radiance per camera system can be determined. Second, a direct conversion factor from relative irradiance of camera 1 to relative irradiance of camera 2 could be determined, directly mapping the sensor irradiance values. The advantage of the first method is the possibility of getting real physical radiance values. For some simulation steps this could be necessary or yield better results. We chose to take the second method of direct mapping since we are not currently using absolute radiance values in our simulation. Furthermore, that way we are not inducing new uncertainties through the calibration with another measurement device. The disadvantage is, that the direct mapping between camera systems is only valid for fixed aperture and color balance values.

To find the scaling factors for converting irradiance of camera 1 to camera 2, the following method can be applied. A series of color patches sampled throughout the RGB space is prepared. The exact color values of the patches are not important. With each camera system that shall be calibrated, multiple images of the calibration patches are taken at different exposure values. We gain a matching of pixel values $Z_{[r|g|b],j}$ in each color channel. These can be converted to relative irradiance values

$$E_{[r|g|b],i} = \frac{f^{-1}(Z_{[r|g|b],j})}{\Delta t_j} \quad (7)$$

of camera i . These correspondences could be used to calculate a per-channel calibration factor from camera i to camera j . However, it has shown to be problematic to only use per-channel color information in this step. Optical sensors are sensitive to light in a relatively large area of the visible spectrum. The color channels are overlapping to some extent, i.e. the irradiance of the red channel includes some irradiance of the greenish spectrum and vice versa. During our tests, it has shown to be more robust to compensate for this effect by including all the color information into a set of linear equations. By solving the linear system of equations

$$E_i * a = E_{i'} \quad (8)$$

in a least squares sense, we obtain the solution vector a . Matrices E_i row-wise contain the sensor irradiance values of all color channels of camera i . The solution vector models a dependency of each color channel of camera i' of all color channels of camera i and yields the appropriate conversion factors as a linear combination. We receive a new set of equations for that task:

$$E_{r,i'}(x) = a_{1,1} * E_{r,i} + a_{2,1} * E_{g,i} + a_{3,1} * E_{b,i} \quad (9)$$

$$E_{g,i'}(x) = a_{1,2} * E_{r,i} + a_{2,2} * E_{g,i} + a_{3,2} * E_{b,i} \quad (10)$$

$$E_{b,i'}(x) = a_{1,3} * E_{r,i} + a_{2,3} * E_{g,i} + a_{3,3} * E_{b,i} \quad (11)$$

These equations model the conversion of sensor irradiance between cameras, accounting for the channel interdependencies. After this step, the camera calibration step has been finished and the simulation of the imaging process with the response characteristics of a camera other than the one the original scene has been recorded with can be done.

C. Changing scene properties in irradiance space

A nice side effect of the return to the irradiance space is the possibility of the elegant modification of scene brightness and contrast. The irradiance space is unbounded and does not suffer from saturation and loss of information. If the original scene has been recorded with full available scene information, it is now possible to easily adapt the scene with respect to brightness and contrast and then remap to the pixel space of a virtual camera. Some of the more complex simulation tasks need those kind of basic operations to yield realistic results. Rain simulation, for example, can only be

realistic if the typically low brightness and contrast of those scenes can be simulated, too.

IV. RESULTS

To verify the correctness of the color processing simulation, we have applied the calibration process to two test cameras. The first camera is our reference system for the simulation environment. It is a Point Grey Bumblebee XB3, a camera system capable of sensing in stereo with a resolution of 1280 x 960 pixels. The camera is supplied with a software development kit, allowing direct control of many important parameters. The second camera is a Sony $\alpha 37$ DSLR with a resolution of 4912 x 3264 pixels. In manual mode, this camera allows a direct setting of all important parameters. The camera has been equipped with a Minolta 24 mm lens. We chose two very different camera systems for this verification step to test the robustness of the simulation process.

Figure 3 shows the color-balance-calibrated response curves of the two cameras at fixed white balance settings. It shows the mapping of pixel values to log exposure and has been created by using the method of [13] for each color channel and then calibrating the color channels relative to each other as described above. At first glance, it is easy to see the different characteristics. The Bumblebee XB3 has a near-linear behaviour in all color channels, whereas the $\alpha 37$ has some clear nonlinear responses especially in the lower and upper areas of exposure. The second curve looks much more bumpy than the first one - the uncertainties should be bigger here. Both cameras respond much stronger to illumination in the blue spectrum than in the red or green spectrum.

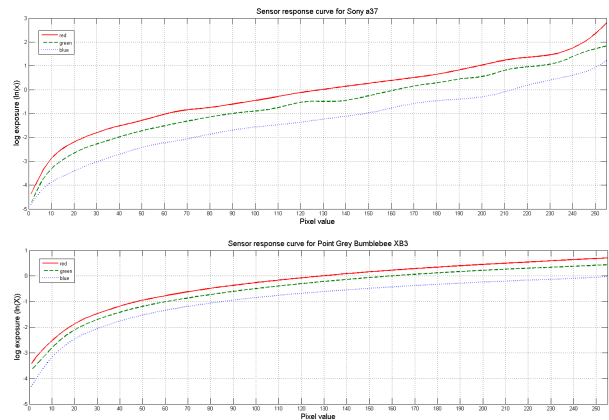


Fig. 3. Response curves with fixed white balance values (BB XB3: [Red: 500; Blue: 800] and $\alpha 37$: "cold white")

To verify the camera-internal behaviour when simulating different exposure times, we recorded 9 gray values as ground truth. The simulation of exposure times can be done by addition in the log exposure space. The red channel has been selected as the reference channel and the other channels have been calculated by adding the red channel difference to them. The red channel error therefore is always 0. The mean and standard deviations of this simulation are shown in table

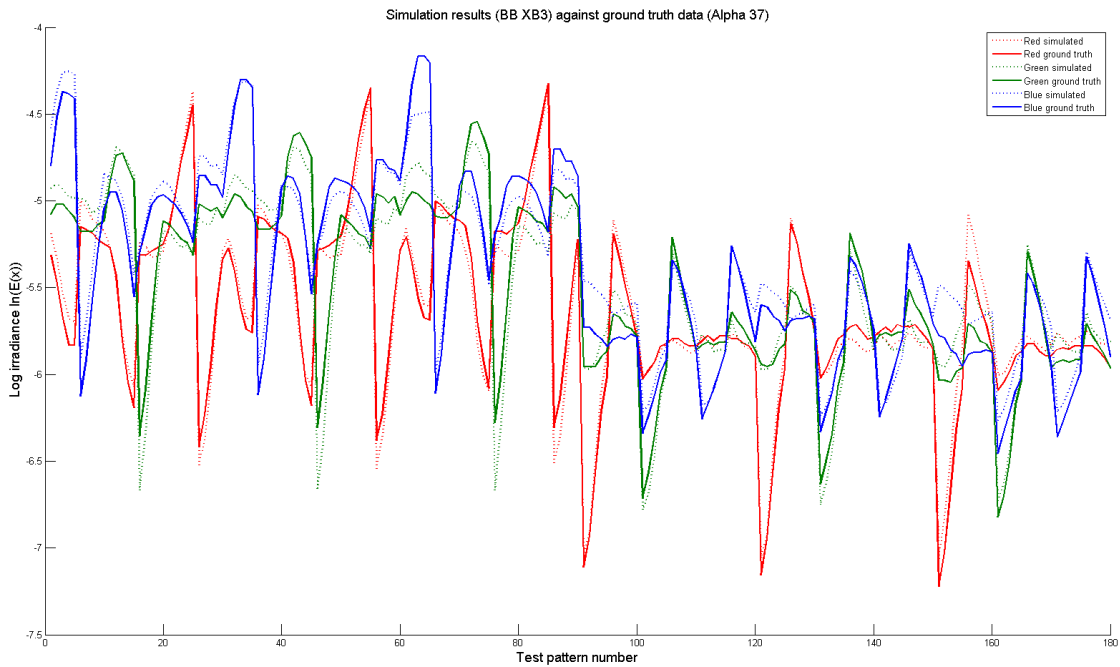


Fig. 4. Simulation results against ground truth

I. As you may notice, the standard deviations lie within a few pixels.

Camera	$\mu(\text{Diff})$ [R,G,B]	$\sigma(\text{Diff})$ [R,G,B]	$\max(\text{Diff})$ [R,G,B]
BB XB3	0, -0.89, 3.78	0, 1.45, 6.67	0, -3, -11
$\alpha 37$	0, 2.33, 4.56	0, 2.45, 5.05	0, 8, 15

TABLE I
RESULTS OF THE CAMERA INTERNAL SIMULATIONS

As a first result of the second calibration step, the intra-camera calibration, we obtained the following irradiance conversion factors for conversions from bumblebee to $\alpha 37$:

$$a_{bb \rightarrow \alpha 37} = \begin{pmatrix} 0.29 & -0.07 & -0.03 \\ -0.03 & 0.45 & -0.05 \\ -0.06 & -0.12 & 0.41 \end{pmatrix}$$

Notable is the clear influence of the blue spectrum on the sensed green irradiance, whereas the red and blue channels are relatively independent. These interdependencies have to be taken into account.

To further verify the correctness of the color simulation, we prepared 30 color test patterns each equally sampled from the RGB and CYMK space. Each test pattern has been recorded at three different exposure times, yielding 180 ground truth correspondences. Figure 4 displays the log irradiance simulation results (dashed lines) in comparison to the ground truth (continuous lines). These results have been generated using equations 5, 6 and 7 to gain the irradiance values for the BB XB3 (the reference system) and then equations 9, 10 and 11 to obtain the simulated irradiances of

the $\alpha 37$. The remapping into pixel space is straightforward then.

Figure 4 shows clear similarity between the simulation and real data. The green channel suffers from a few big outliers at the extreme values of irradiance. If the irradiance in the green channel is low, the error of the simulation rises. This is the result of the big uncertainties around the extrema together with the high interdependency of the green channel. In the blue channel most outliers are due to saturation of the ground truth data (e.g. the one at test pattern 60). Table II shows mean and standard deviations of the simulation. Although the maximum deviations are a bit high, mean and standard deviations show good approximation of the simulation results.

$\mu(\text{Diff})$ [R,G,B]	$\sigma(\text{Diff})$ [R,G,B]	$\max(\text{Diff})$ [R,G,B]
0.54, -0.19, 2.83	5.81, 7.38, 8.29	17, 20, 23

TABLE II
RESULTS OF THE SIMULATION OF $\alpha 37$ COLORS WITH BB XB3 IMAGES

To evaluate the behaviour of an ADAS on simulated data, we recorded a scene with approximately 6000 frames of german traffic signs and calculated the rate of correct recognition and the rate of false positives with the two camera systems. The cameras have been mounted as close to each other as possible. The TSR algorithm is an in-house developed application which provides basically three steps to recognize a traffic sign: First a hough transformation is applied to find circular areas, second the image is segmented and third a support vector machine classifies the image

segment. Since it operates on grayscale images only, it is not directly color dependent, but it is sensitive to changing contrast and noise. Along with the ground truth application, we did a simulation of the $\alpha37$ using BB XB3 records. These simulated images have also been applied to the TSR. Table III shows the recognition results. On simulated images, the TSR algorithm has detected about 30 traffic signs fewer than on ground truth images. But the detection rate of the BB XB3, with which the SVM has been trained, is significantly higher than the ground truth of the $\alpha37$ as well as the simulated $\alpha37$ images. Since the simulated images are color-correct but contain a lot more noise from the small BB XB3 sensor, it is not surprising, that the simulation results still differ. The low overall recognition rate of the TSR algorithm is because of the limitation of its hough transform step to a fixed circle radius for performance reasons.

	BB XB3	$\alpha37$	BB XB3 \rightarrow $\alpha37$
Matches	244	113	79
Mismatches	55	47	42

TABLE III
RESULTS OF THE TSR ON GROUND TRUTH AND SIMULATED DATA

V. CONCLUSION

We presented a method to calibrate two optical systems in terms of color correctness and evaluated the differences of the simulation to ground truth data. We have shown how to apply the simulation to an ADAS to derive statements towards its robustness under varying conditions. The results of the color simulation still suffers from two problems: in the areas of extremely high or low irradiance values the simulation yields high differences to ground truth data since the response curves of the camera systems are highly dynamic in these areas. The second problem occurs, whenever the reference systems pixel values go into saturation. If this happens, data is lost and the simulation cannot find the correct irradiance values. In the non-saturated areas of sensor irradiance the results are lying within a few pixels to the ground truth. To cope with these problems, RAW sensor data could be used to gain a higher values margin. Using e.g. 16 bit per color channel prevents the irradiance values from going into saturation too early, which should result in more precise simulation results. Unfortunately, our reference system does not support streaming of 16 bit stereo RAW data via its API. Another difficulty is the interdependency of the parameters, such as gain, noise and color output. To further improve the color simulation, the other parts need to be simulated as well.

VI. FUTURE WORK

As color correctness is only one necessary parameter to consider at the subject of simulating a whole optical sensor, the next steps are to find suitable simulations for the other parameters and verify them against ground truth. We are

currently working on improvements of the simulation. The focus lies on finding simulation parameters that lead to the same effects as real data in the ADAS testing algorithms.

ACKNOWLEDGMENT

This work was partially funded by the State of Baden Wuerttemberg, Germany, Ministry of Science, Research and Arts within the scope of Cooperative Research Training Group. Additionally, it has been partially supported by the German Ministry of Science and Education (BMBF) in the project EffektiV under grant 01IS13022.

REFERENCES

- [1] N. Bannow, M. Becker, O. Bringmann *et al.*, "Safety Evaluation of Automotive Electronics Using Virtual Prototypes: State of the Art and Research Challenges," in *DAC 2014*, 2014.
- [2] S. Maldonado-Bascon, S. Lafuente-Arroyo, P. Gil-Jimenez, H. Gomez-Moreno, and F. Lopez-Ferreras, "Road-Sign Detection and Recognition Based on Support Vector Machines," *IEEE Transactions on Intelligent Transportation Systems*, vol. 8, no. 2, pp. 264–278, Jun. 2007.
- [3] C. Bahlmann, Y. Zhu, M. Pellkofer, and T. Koehler, "A system for traffic sign detection, tracking, and recognition using color, shape, and motion information," *Intelligent Vehicles Symposium*, pp. 255–260, 2005.
- [4] A. Geiger, P. Lenz, and R. Urtasun, "Are we ready for autonomous driving? The KITTI vision benchmark suite," *2012 IEEE Conference on Computer Vision and Pattern Recognition*, pp. 3354–3361, Jun. 2012.
- [5] J. Stallkamp and M. Schlipsing, "The German traffic sign recognition benchmark: a multi-class classification competition," *International Joint Conference on Neural Networks (IJCNN)*, pp. 1453–1460, 2011.
- [6] H. Ishida, T. Takahashi, I. Ide, Y. Mekada, and H. Murase, "Generation of Training Data by Degradation Models for Traffic Sign Symbol Recognition," *IEICE TRANSACTIONS on Information and Systems*, no. 8, pp. 1134–1141, 2007.
- [7] H. Hoessler, C. Wöhler, F. Lindner, and U. Kreß el, "Classifier training based on synthetically generated samples," in *The 5th International Conference on Computer Vision Systems*, 2007.
- [8] E. A. Lee, "Cyber physical systems: Design challenges," EECS Department, University of California, Berkeley, Tech. Rep., Jan 2008.
- [9] W. Mueller, M. Becker, A. Elfeky, and A. DiPasquale, "Virtual prototyping of Cyber-Physical Systems," *17th Asia and South Pacific Design Automation Conference*, pp. 219–226, Jan. 2012.
- [10] S. Reiter, M. Pressler, A. Viehl, O. Bringmann, and W. Rosenstiel, "Reliability assessment of safety-relevant automotive systems in a model-based design flow," *18th Asia and South Pacific Design Automation Conference (ASP-DAC)*, pp. 417–422, Jan. 2013.
- [11] J. Kajiya, "The rendering equation," *ACM Siggraph Computer Graphics*, vol. 20, no. 4, pp. 143–150, 1986.
- [12] S. J. Gortler, R. Grzeszczuk, R. Szeliski, and M. F. Cohen, "The lumigraph," *Proceedings of the 23rd annual conference on Computer graphics and interactive techniques - SIGGRAPH '96*, pp. 43–54, 1996.
- [13] P. E. Debevec and J. Malik, "Recovering high dynamic range radiance maps from photographs," in *Proceedings of the 24th Annual Conference on Computer Graphics and Interactive Techniques*, ser. SIGGRAPH '97, 1997, pp. 369–378.
- [14] C. Kolb, D. Mitchell, and P. Hanrahan, "A realistic camera model for computer graphics," *Proceedings of the 22nd annual conference on Computer graphics and interactive techniques - SIGGRAPH '95*, pp. 317–324, 1995.
- [15] P. Debevec, "Rendering synthetic objects into real scenes: Bridging traditional and image-based graphics with global illumination and high dynamic range photography," *ACM SIGGRAPH 2008 classes*, 2008.
- [16] I. Sato, Y. Sato, and K. Ikeuchi, "Acquiring a radiance distribution to superimpose virtual objects onto a real scene," *IEEE Transactions on Visualization and Computer Graphics*, vol. 5, no. 1, pp. 1–12, 1999.
- [17] Y. Yu and J. Malik, "Recovering photometric properties of architectural scenes from photographs," *Proceedings of the 25th annual conference on Computer graphics and interactive techniques - SIGGRAPH '98*, pp. 207–217, 1998.